Heliyon 5 (2019) e02545

Contents lists available at ScienceDirect

Heliyon

journal homepage: www.heliyon.com

Effect of CO adsorption on properties of transition metal doped porphyrin: A DFT and TD-DFT study

H.Y. Ammar [a,b,*], H.M. Badran [a,b]

[a] Physics Department, College of Science & Arts, Najran University, P. O. 1988, Najran, Saudi Arabia
[b] Physics Department, Faculty of Education, Ain Shams University, Roxy, Cairo, Egypt

ARTICLE INFO

Keywords:
Molecular physics
Theoretical chemistry
Adsorption
CO
Porphyrin
DFT
TD-DFT
UV-Vis. spectrum
Transition metal

ABSTRACT

The structural, electronic and optical properties of transition metal doped porphyrin (TM@P; TM = Mn, Co, Fe, Cu, Ni, Zn) as well as the effect of CO adsorption on TM@P properties have been investigated using the density functional theory (DFT). The presented results include adsorption energies, bond lengths, electronic configurations, magnetic moments, density of states, frontier molecular orbitals, and UV-Vis. spectra. Our calculation results show that, the CO molecule favors to be adsorbed on TM-doped Porphyrin with its carbon head. The most energetically stable adsorption of CO is reported for Fe doped Porphyrin. The interaction between CO molecules with TM@P is attributed to donation-back donation as well as charge transfer mechanisms. Mn, Co and Fe-doped porphyrins have visible active nature which may be affected by CO adsorption, whereas, Ni, Cu and Zn-doped porphyrins have UV active nature which not affected by CO adsorption. These results may be meaningful for CO removal and detection.

1. Introduction

Carbon monoxide (CO) is a colorless odorless toxic gas, which harms human due to its high binding ability with hemoglobin [1]. CO is widely produced from automotive engines and industrial combustion systems. It is one of the most air pollutants. Thus, in order to reduce environmental pollution, it is necessary to use catalysts/sorbents to detect, remove or trap the carbon monoxide [2, 3].

Porphyrins are a class of naturally occurring macrocyclic compounds [4]. They possess a large-conjugated system, interesting aggregation properties and show potential applications in various fields [5], including charge separation, molecular electronics, transport of oxygen, photovoltaics biocatalysis, play an important role in the metabolism of living organisms [6], widely utilized as the UV–Vis [7] and photoelectrochemical sensors [8, 9].

Although porphyrin and its derivatives are widely studied, there are little studies for its transition metal doped complexes except for iron [10, 11]. Roy et. al [12]. have studied non-linear optical properties of transition metal (Fe, Co and Ni) doped porphyrin and the optical activity in cobalt porphyrin in the light of infrared (IR) and Raman spectroscopy. Paul et al. [13] found that a very low concentration of iron porphyrin could enhance the sensitivity of virgin polypyrrole to carbon monoxide detection at very low ppm level under ambient conditions and without any external agent. On the other hand, porphyrins can be adequately used as coating of conductive substrates such as carbon nanotubes or semiconductor nanostructures [14]. Mosciano et al. [15] found that porphyrins coated metal oxides (ZnO) could lead to a new class of photo-activated sensors to carbon monoxide. Chang et. al [16]. have studied the adsorption of NO, CO and O_2 molecules on Co doped tetraphenylporphyrin on Au(111), Ag(111), and Cu(111). They found that the CO is almost vertically attached onto the CoTPP/metal substrate. Lian et. al [17]. have reported that trimethylamine functionalized iron tetraphenylporphyrin catalysts is able to photoreduce CO2 to CO in water. Shah et. al [18]. have studied the structural, electronic, spectroscopic, and optical properties of TM dopd TPP (TM = Fe, Co, Ni, Cu, and Zn) and concluded that Co and Cu doped TPP are visible active materials and may be used for optoelectronic applications.

Liao and Scheiner [19] illustrated that the presence of ligand such as CO molecule induced perturbation of the electronic structure of iron and cobalt porphyrins that may lead to considerable changes in their electronic and optical properties.

In the present work, the structural stabilities, electronic and optical properties of TM-doped porphyrin (TM = Mn, Co, Fe, Cu, Ni and Zn) were investigated using density functional theory (DFT) method. As well as the

* Corresponding author.
E-mail address: hyammar@hotmail.com (H.Y. Ammar).

https://doi.org/10.1016/j.heliyon.2019.e02545
Received 2 March 2019; Received in revised form 22 August 2019; Accepted 26 September 2019

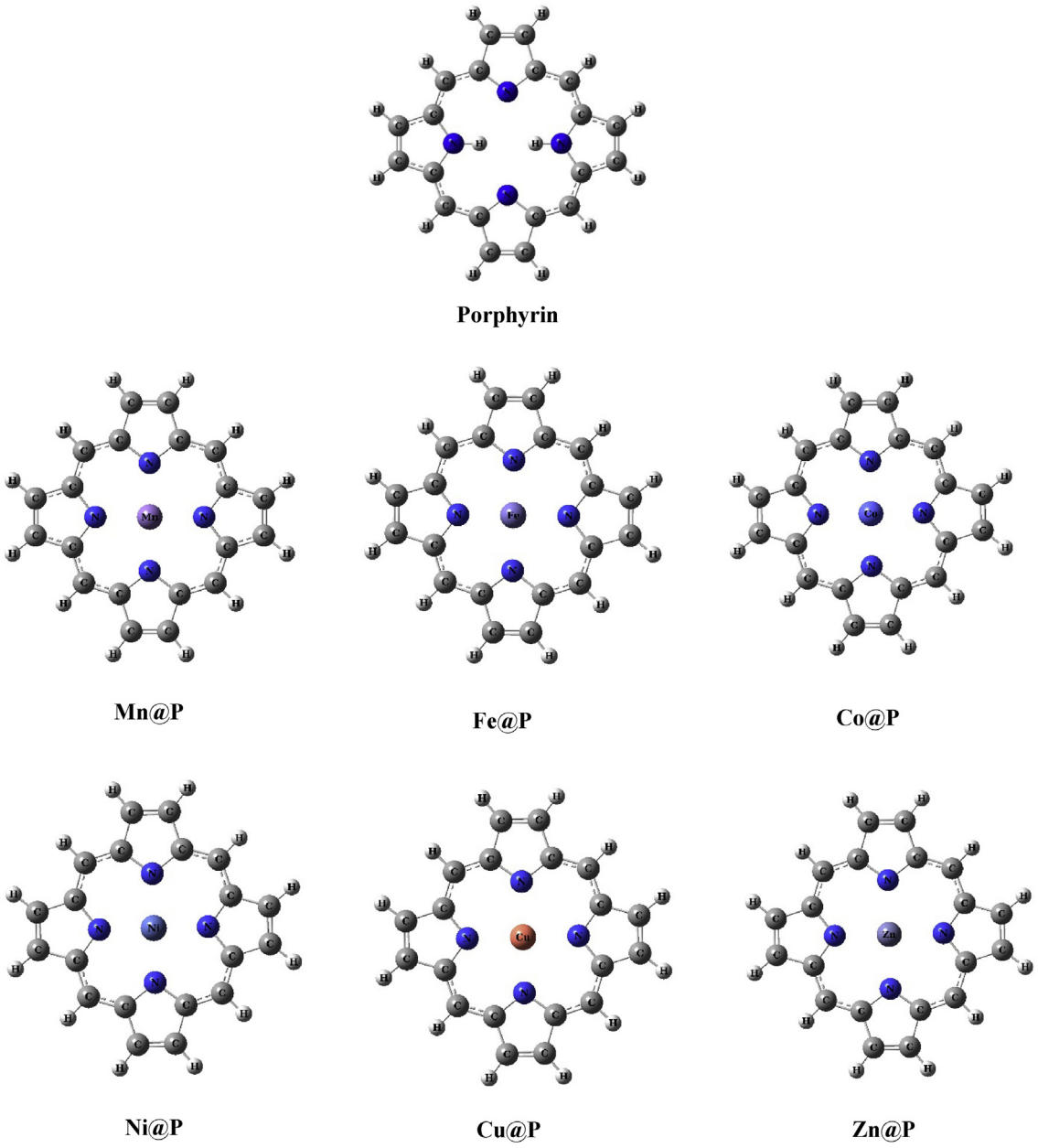

Fig. 1. The optimized structures for Porphyrin and TM@P, calculated at B3LYP/LanL2DZ.

Table 1
Properties of P and TM@P. Bond lengths (d, Å), Ionization potential (I.P., eV), electron affinity (E.A., eV), HOMO and LUMO energy levels (eV), hardness (η, eV), Binding energy (E_b,eV), NBO charges (Q, |e|), the dipole moment (D, Debye) and the magnetic moment (μ, μ_B).

	P		Mn@P		Fe@P		Co@P		Ni@P		Cu@P		Zn@P	
	LanL2DZ	6-31G(d)	LanL2DZ	6-31G(d)	LanL2DZ	6-31G(d)	LanL2DZ	6-31G(d)	LanL2DZ	6-31G(d)	LanL2DZ	6-31G(d)	LanL2DZ	6-31G(d)
d_{TM-N}	-	-	2.016	1.998	2.008	1.990	1.998	1.975	1.984	1.958	2.031	2.005	2.069	2.040
d_{C-N}	1.387	1.372	1.401	1.387	1.397	1.381	1.397	1.379	1.397	1.379	1.393	1.375	1.391	1.373
I.P.	5.375	5.148	5.485	5.183	5.508	5.186	5.478	5.171	5.510	5.207	5.477	5.202	5.395	5.209
E.A.	2.548	2.239	2.443	2.118	2.388	2.062	2.378	2.034	2.404	2.066	2.454	2.119	2.453	2.098
$E_{HOMO-LUMO}$	2.827	2.910	3.042	3.065	3.120	3.124	3.099	3.137	3.105	3.140	3.023	3.084	2.943	3.115
η	1.413	1.455	1.521	1.532	1.560	1.562	1.550	1.569	1.553	1.570	1.512	1.542	1.471	1.557
E_b	-4.977	-5.216	-5.112	-5.329	-5.096	-5.354	-5.094	-5.363	-5.126	-5.382	-5.047	-5.377	-5.036	-5.316
Q_N	-0.404	-0.550	-0.634	-0.638	-0.605	-0.611	-0.599	-0.587	-0.579	-0.567	-0.645	-0.611	-0.724	-0.653
Q_{TM}	-	-	1.056	1.392	0.905	1.181	0.854	1.076	0.735	0.939	1.014	1.114	1.393	1.283
D	0.000	0.001	0.001	0.000	0.001	0.001	0.000	0.001	0.001	0.000	0.000	0.000	0.000	0.000
μ	0.000	0.000	3.22	3.42	2.07	2.00	1.03	0.99	0.000	0.000	0.59	0.71	0.000	0.000

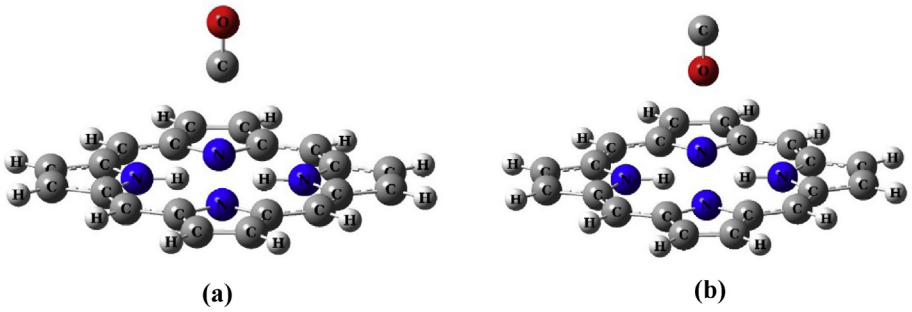

Fig. 2. The optimized structures for CO/P complex, calculated at B3LYP/LanL2DZ. (a) mode 1, and (b) mode 2.

Table 2
Adsorption properties of CO on P. Adsorption energies ($E_{ads.}$, eV), bond lengths (d, Å), NBO charges (Q, |e|), HOMO and LUMO energy levels (eV), and the dipole moment (D, Debye).

Mode	Type	E_{ads}		$d_{C\text{-}O}$		$d_{CO\text{-}P}$		Q_{CO}		HOMO		LUMO		$E_{HOMO\text{-}LUMO}$		D	
		LanL2DZ	6-31G(d)	LanL2DZ	6-31G(d)	LanL2DZ	6-31G(d)	LanL2DZ	6-31G(d)	LanL2DZ	6-31G(d)	LanL2DZ	6-31G(d)	LanL2DZ	6-31G(d)	LanL2DZ	6-31G(d)
1	CO/P	-0.166	-0.017	1.167	1.139	3.023	3.098	-0.002	-0.002	-5.369	-5.142	-2.557	-2.235	2.812	2.907	0.222	0.094
2	CO/P	-0.113	-0.012	1.165	1.137	3.096	2.885	0.000	0.000	-5.364	-5.149	-2.542	-2.237	2.822	2.912	0.071	0.174

effect of adsorption of carbon monoxide molecule on TM-doped porphyrin was studied.

2. Methods

To investigate the adsorption characteristics of CO on TM@P, DFT [20] methods were performed at B3LYP/LanL2dz and B3LYP/6-31G(d) levels of theory for the calculations of the adsorbate-substrate interactions. Full geometric optimizations were done for porphyrin (P), TM-doped Porphyrin (TM@P), free CO molecule, CO/P complex and CO/TM@P. To obtain the most energetic stable geometrical structure for P, TM@P, CO/P and CO/TM@P, we begin our optimizations for each structure with the lowest possible spin states, S = 0 or 1/2 for even and odd count electron structure, respectively. Then optimization process was repeated at the higher spin states gradually until reaching the optimum spin state for the structure. All calculations were done using Gaussian09 suite of program [21]. Densities of states (DOS) for adsorbate and complex systems were visualized using GaussSum3.0 program [22], Full natural bond orbital (NBO) analysis were made to calculate the charge distribution for substrates, adsorbates and complex systems by using NBO version 3.1 [23]. Time dependent DFT (TD-DFT) calculations were performed for P, TM@P, CO/P, and CO/TM@P complexes to simulate their UV-Vis absorption spectra.

The ionization potential (IP) and electron affinity (EA) are expressed in terms of the highest occupied molecular orbital (HOMO) and the lowest unoccupied molecular orbital (LUMO) according to Koopmans' approximation [12] as:

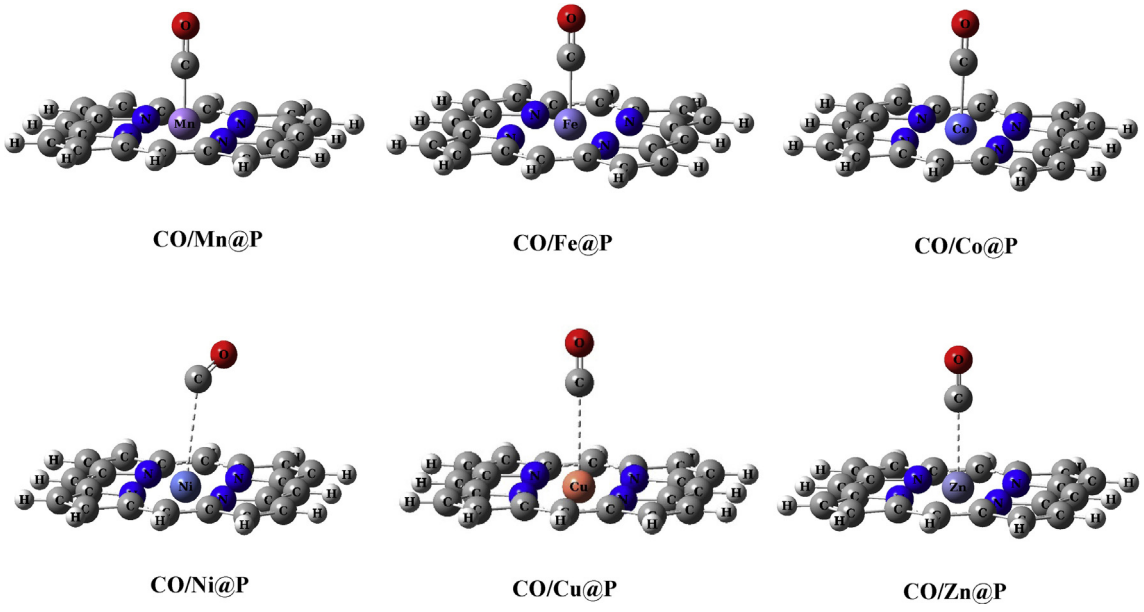

Fig. 3. The optimized structures for the CO/TM@P for mode 1, calculated at B3LYP/LanL2DZ.

Table 3
Adsorption properties of CO on TM@P. Adsorption energies ($E_{ads.}$, eV), bond lengths (d, Å), HOMO and LUMO energy levels (eV), the dipole moment (D, Debye) and the magnetic moment (μ, μ_B).

Mode	Type	E_{ads}		$d_{C\text{-}O}$		$d_{CO\text{-}TM}$		HOMO		LUMO		$E_{HOMO\text{-}LUMO}$		D		μ	
		LanL2DZ	6-31G(d)	LanL2DZ	6-31G(d)	LanL2DZ	6-31G(d)	LanL2DZ	6-31G(d)	LanL2DZ	6-31G(d)	LanL2DZ	6-31G(d)	LanL2DZ	6-31G(d)	LanL2DZ	6-31G(d)
	CO/Mn@P	-0.468	-0.408	1.182	1.159	1.763	1.742	-5.637	-5.322	-2.490	-2.176	3.147	3.146	1.776	1.744	1.19	1.23
	CO/Fe@P	-1.042	-0.756	1.176	1.153	1.743	1.718	-5.586	-5.269	-2.443	-2.124	3.144	3.145	1.121	1.125	0.00	0.00
	CO/Co@P	-0.334	-0.429	1.165	1.141	2.045	1.950	-5.302	-4.980	-2.418	-2.103	2.884	2.877	0.127	0.145	0.92	0.93
1	CO/Ni@P	-0.102	-0.083	1.166	1.138	3.225	3.230	-5.517	-5.218	-2.420	-2.084	3.097	3.134	0.243	0.059	0.00	0.00
	CO/Cu@P	-0.132	-0.078	1.164	1.137	3.050	3.223	-5.436	-5.177	-2.439	-2.098	2.997	3.079	0.176	0.412	0.61	0.72
	CO/Zn@P	-0.206	-0.145	1.161	1.134	2.656	2.686	-5.307	-5.107	-2.430	-2.087	2.878	3.019	0.628	1.119	0.00	0.00
	CO/Mn@P	-0.130	-0.093	1.163	1.138	2.678	2.938	-5.431	-5.157	-2.417	-2.109	3.014	3.048	0.421	0.393	3.27	3.46
	CO/Fe@P	-0.113	0.076	1.162	1.138	2.654	2.987	-5.457	-5.159	-2.361	-2.040	3.096	3.119	0.316	0.315	2.08	2.02
2	CO/Co@P	-0.122	-0.070	1.162	1.138	2.595	3.012	-5.420	-5.151	-2.349	-2.018	3.071	3.133	0.373	0.263	1.01	1.00
	CO/Ni@P	-0.056	-0.044	1.163	1.137	3.256	3.575	-5.484	-5.196	-2.386	-2.059	3.098	3.137	0.111	0.067	0.00	0.00
	CO/Cu@P	-0.086	-0.053	1.163	1.138	2.936	3.318	-5.439	-5.188	-2.431	-2.109	3.008	3.080	0.223	0.158	0.59	0.72
	CO/Zn@P	-0.131	-0.072	1.163	1.138	2.610	3.062	-5.323	-5.179	-2.412	-2.113	2.911	3.066	0.621	0.400	0.00	0.00

Table 4
Adsorption properties of CO on TM@P. NBO charges (Q, |e|).

Mode	Type	Q_C			Q_O			Q_{CO}			Q_{TM}			SD		
		LanL2DZ	6-31G(d)	6-311G(d)	LanL2DZ	6-31G(d)	6-311G(d)	LanL2DZ	6-31G(d)	6-311G(d)	LanL2DZ	6-31G(d)	6-311G(d)	LanL2DZ	6-31G(d)	6-311G(d)
	CO/Mn@P	0.770	0.498	0.462	-0.471	-0.476	-0.465	0.300	0.022	-0.004	0.257	0.905	1.126	1.228	1.235	1.229
	CO/Fe@P	0.816	0.554	0.514	-0.455	-0.463	-0.451	0.361	0.091	0.062	0.142	0.777	1.014	0.000	0.000	0.000
	CO/Co@P	0.659	0.553	0.410	-0.447	-0.447	-0.431	0.212	0.106	-0.021	0.496	0.799	1.253	0.985	1.011	1.009
1	CO/Ni@P	0.529	0.529	0.458	-0.496	-0.500	-0.468	0.033	0.029	-0.010	0.704	0.935	1.181	0.000	0.000	0.000
	CO/Cu@P	0.554	0.552	0.470	-0.488	-0.493	-0.461	0.067	0.058	0.009	0.967	1.103	1.403	0.593	0.677	0.664
	CO/Zn@P	0.561	0.587	0.464	-0.511	-0.461	-0.442	0.050	0.126	0.021	1.372	1.199	1.652	0.000	0.000	0.000
	CO/Mn@P	0.550	0.548	0.517	-0.499	-0.514	-0.530	0.051	0.033	-0.013	1.026	1.400	1.384	3.372	3.361	3.490
	CO/Fe@P	0.540	0.539	0.537	-0.488	-0.508	-0.520	0.052	0.031	0.017	0.859	1.175	1.297	2.158	2.164	
2	CO/Co@P	0.545	0.533	0.490	-0.489	-0.507	-0.484	0.057	0.026	0.006	0.804	1.078	1.306	1.079	1.138	1.110
	CO/Ni@P	0.503	0.509	0.464	-0.485	-0.501	-0.463	0.017	0.008	0.001	0.732	0.949	1.176	0.000	0.000	0.000
	CO/Cu@P	0.520	0.519	0.478	-0.489	-0.503	-0.475	0.031	0.016	0.003	0.999	1.125	1.401	0.590	0.673	0.657
	CO/Zn@P	0.561	0.535	0.497	-0.511	-0.508	-0.491	0.050	0.027	0.005	1.372	1.291	1.659	0.000	0.000	0.000

Table 5
Electronic configurations of TM as well as, C and O atoms of CO for free CO molecule, TM@P, and CO/TM@P complexes for adsorption mode 1.

Type	TM						C						O					
	4s			3d			2s			2p			2s			2p		
	LanL2DZ	6-31G(d)	6-311G(d)	LanL2DZ	6-31G(d)	6-311G(d)	LanL2DZ	6-31G(d)	6-311G(d)	LanL2DZ	6-31G(d)	6-311G(d)	LanL2DZ	6-31G(d)	6-311G(d)	LanL2DZ	6-31G(d)	6-311G(d)
CO	-			-			1.69	1.67	1.64	1.78	1.79	1.84	1.77	1.74	1.73	4.72	4.73	4.73
Mn@P	0.24	0.20	0.28	5.44	5.19	5.17	-	-	-	-	-	-	-	-	-	-	-	-
Fe@P	0.24	0.31	0.28	6.58	6.24	6.38	-	-	-	-	-	-	-	-	-	-	-	-
Co@P	0.24	0.31	0.28	7.61	7.29	7.42	-	-	-	-	-	-	-	-	-	-	-	-
Ni@P	0.30	0.43	0.37	8.67	8.31	8.46	-	-	-	-	-	-	-	-	-	-	-	-
Cu@P	0.31	0.41	0.37	9.35	9.14	9.23	-	-	-	-	-	-	-	-	-	-	-	-
Zn@P	0.31	0.44	0.40	9.97	9.91	9.94	-	-	-	-	-	-	-	-	-	-	-	-
CO/ Mn@P	0.28	0.33	0.31	6.01	5.32	5.55	1.15	1.21	1.26	2.04	2.23	2.21	1.73	1.70	1.70	4.73	4.74	4.75
CO/ Fe@P	0.29	0.33	0.31	7.09	6.44	6.66	1.14	1.20	1.25	2.00	2.19	2.17	1.73	1.70	1.70	4.72	4.73	4.73
CO/ Co@P	0.28	0.34	0.30	7.70	7.27	7.43	1.42	1.37	1.49	1.87	2.01	2.02	1.74	1.71	1.71	4.70	4.71	4.71
CO/ Ni@P	0.30	0.42	0.36	8.67	8.31	8.45	1.66	1.63	1.64	1.77	1.80	1.85	1.76	1.73	1.73	4.73	4.73	4.73
CO/ Cu@P	0.31	0.40	0.36	9.35	9.14	9.23	1.64	1.62	1.63	1.76	1.79	1.85	1.76	1.74	1.73	4.72	4.73	4.72
CO/ Zn@P	0.32	0.43	0.40	9.97	9.91	9.94	1.58	1.55	1.60	1.80	1.82	1.88	1.76	1.73	1.72	4.69	4.70	4.71

$$IP \approx -E_{HOMO} \tag{1}$$

$$EA \approx -E_{LUMO} \tag{2}$$

The chemical hardness (**η**), a quantum parameter introduced by Pearson to account the stability of the compound, can be expressed in terms of HOMO and LUMO as,

$$\eta \approx \frac{1}{2}(IP - EA) \tag{3}$$

The binding energy per atom (E_b) for porphyrin and TM@P molecules is calculated from Eqs. (4) and (5), respectively.

$$E_b = \frac{E_p - (20E_C + 14E_H + 4E_N)}{total\ number\ of\ atoms} \tag{4}$$

$$E_b = \frac{E_{TM@P} - (20E_C + 12E_H + 4E_N + E_{TM})}{total\ number\ of\ atoms} \tag{5}$$

Where E_p and $E_{TM@P}$ are the total energies of P, TM@P and E_C, E_H, E_N E_{TM} are the atomistic energies for carbon, hydrogen, nitrogen and TM atoms, respectively.

The adsorption energy (E_{ads}) for CO molecule on porphyrin and TM@P molecules is calculated from Eqs. (6) and (7), respectively.

$$E_{ads} = E_{CO/P} - (E_P + E_{CO}) \tag{6}$$

$$E_{ads} = E_{CO/TM@P} - (E_{TM@P} + E_{CO}) \tag{7}$$

Where, $E_{CO/P}$, $E_{CO/TM@P}$, E_{CO} are the energies of the optimized CO/P, CO/TM@P and the free CO molecule, respectively.

3. Results and discussions

3.1. Geometrical optimization of TM@P

A geometrical optimization were done for the porphyrin (P) and TM-doped porphyrin (TM@P); (TM = Mn, Fe, Co, Ni, Cu, and Zn). Fig. 1 represents the optimized structures for P and TM@P. The energetically optimized structures show that both of P and TM@P molecules are planar, matched with Giovannetti [24]. As shown in Table 1, the average bond lengths TM-N are found to be in the range 1.984–2.069Å and 1.958–2.040Å and the average C–N bonds in pyrrole rings are in the range 1.391–1.401Å and 1.373–1.387Å rather than 1.387Å and 1.372 in pare P molecule, for LanL2dz and 6-31G(d) basis sets, respectively. Indicating that the TM atom somewhat increases the compactness of the porphyrin complexes, this is in good agreement with previous literature [12]. The stability of TM@P molecules were studied in terms of ionization potential (IP), electronic affinity (EA), chemical hardness (η), HOMO-LUMO energy gap ($E_{HOMO\text{-}LUMO}$), and the binding energy per atom (E_B). As listed in Table 1, the doping of TM atom in porphyrin increases the IP to the range 5.395–5.510 eV and 5.171–5.209 eV comparing to that of P (5.375 eV and 5.148 eV) for LanL2dz and 6-31G(d) basis sets, respectively, indicating the stability of P and TM@P molecules. On the other hand, the electronic affinity for P decreases from 2.548 eV and 2.239 eV to be for TM@P in the range 2.378–2.454 eV and 2.034–2.119 eV, for LanL2dz and 6-31G(d) basis sets, respectively, indicating the higher reactivity for TM@P molecules than P. Yang et al. [25] reported that the clusters with large $E_{HOMO\text{-}LUMO}$ are more chemically stable. In our case, the doping of TM in porphyrin promotes both of the $E_{HOMO\text{-}LUMO}$ values and the chemical hardness (η) values by the ratio of 4.1–10.4% and 5.3–7.9%, for LanL2dz and 6-31G(d) basis sets, respectively, indicating the stability of TM porphyrin complexes. Furthermore, the TM doping enhances the E_b values by the ratio of 1.2–3.0 % and 1.9–3.2%, for LanL2dz and 6-31G(d) basis sets, respectively, leading to the stability of TM porphyrin complexes. To explain our obtained results, the atomic charge distributions for the investigated

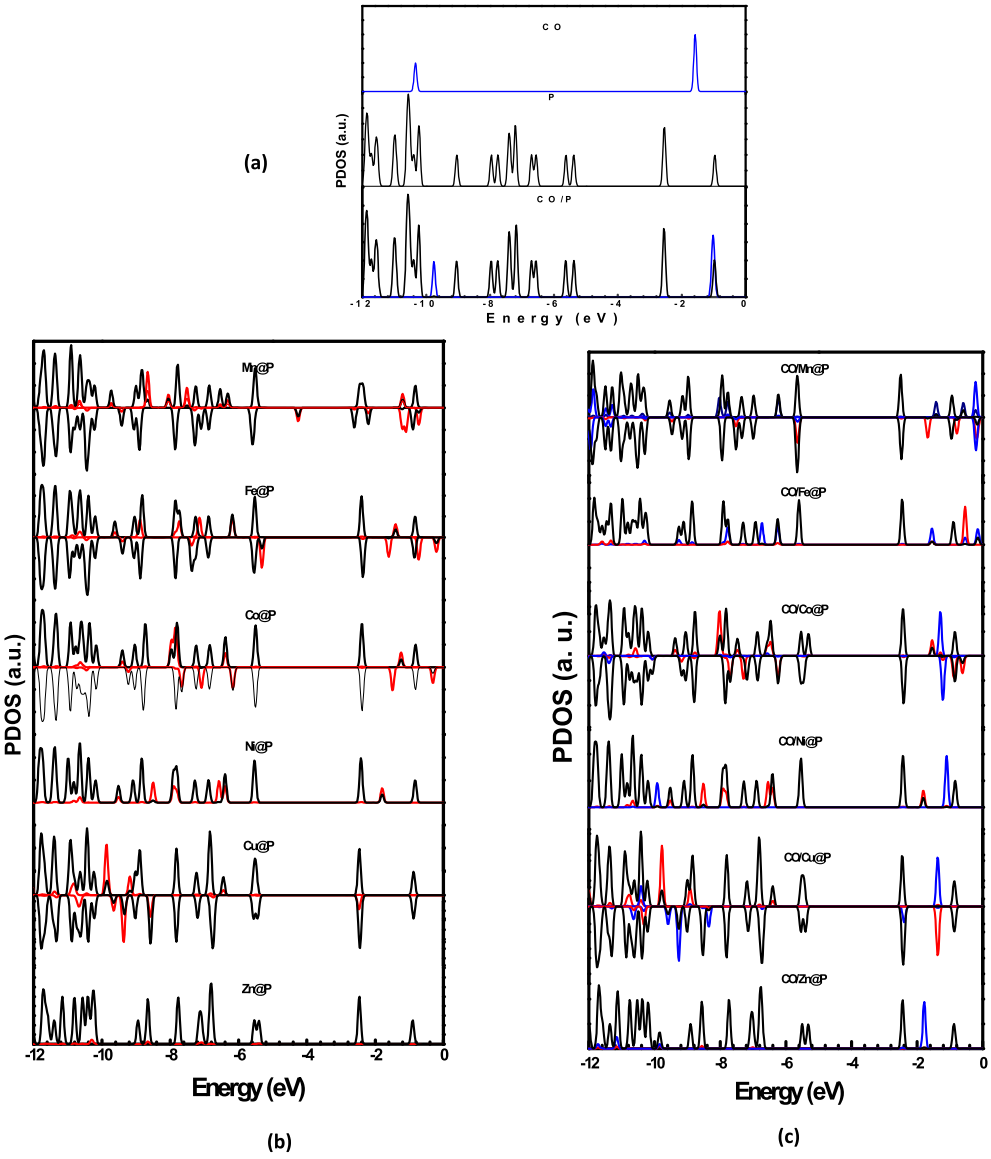

Fig. 4. PDOS calculated at B3LYP/LanL2dz level of theory for (a) free CO, P, CO/P, (b) TM@P and (c) CO/TM@P.

complexes were calculated using natural bond orbital (NBO) calculations. One can observe that, The TM atoms acquire positive charges. In the other hand, the negative charges on the nitrogen atoms in TM@P increase than those in porphyrin molecule. The positive charge acquired on the TM atom is higher than the total increment of the negative charges on the four nitrogen atoms in the TM@P complex. These means there is a charge transfer from the TM to the nitrogen atoms and to the rest of the complex. As a result, the stability of the TM@P complexes maybe referred to the intramolecular charge transfer [26].

3.2. Adsorption of CO on P and TM@P

We suggest two adsorption modes for CO molecule on P to form CO/P. In the first mode CO interacts with porphyrin via its carbon head while, in the second mode CO interacts with porphyrin via its oxygen head, see Fig. 2. Firstly, geometrical optimization were done for the substrates (P) and the gaseous CO molecule. We found that, the bond length C–O for the CO is 1.17 Å and 1.14 Å for LanL2dz and 6-31G(d) basis sets, respectively, this is in good agreement with greenwood [27] and Shalabi et al. [3]. Secondly, the geometrical optimization without any constrains were done for the CO/P. The adsorption energies (E_{ads}) were calculated using Eq. (6). Our results in Table 2 show that, the binding of the CO gas molecules onto the porphyrin in both of adsorption modes is mainly due to electrostatic and van der Waals interactions. The properties of the adsorbed CO remain close to those of the gas phase, where there is no significant change in C–O bond length, the net charge on CO in CO/P approximately equals to zero, and the CO/P HOMO-LUMO energy gap closes to that of bare porphyrin. Assuming a boundary value of 0.21 eV between physical adsorption and chemical adsorption [3], one can say that, the CO adsorption on P is physisorption and the CO molecule prefers to interact with porphyrin molecule via its carbon head where the adsorption energy value for mode 1 is more negative than that for mode 2.

To study the adsorption properties of CO on TM@P, we suggest the same adsorption modes, as discussed previously, for CO molecule on TM@P to form CO/TM@P. A geometrical optimization without any constrains were done for the CO/TM@P. The optimized structures for CO/TM@P for mode 1 are shown in Fig. 3. The adsorption energies (E_{ads}) were calculated using Eq. (7). Looking to Table 3, one can notice that, there is no significant change in CO bond length ($d_{C\text{-}O}$). The E_{ads} values

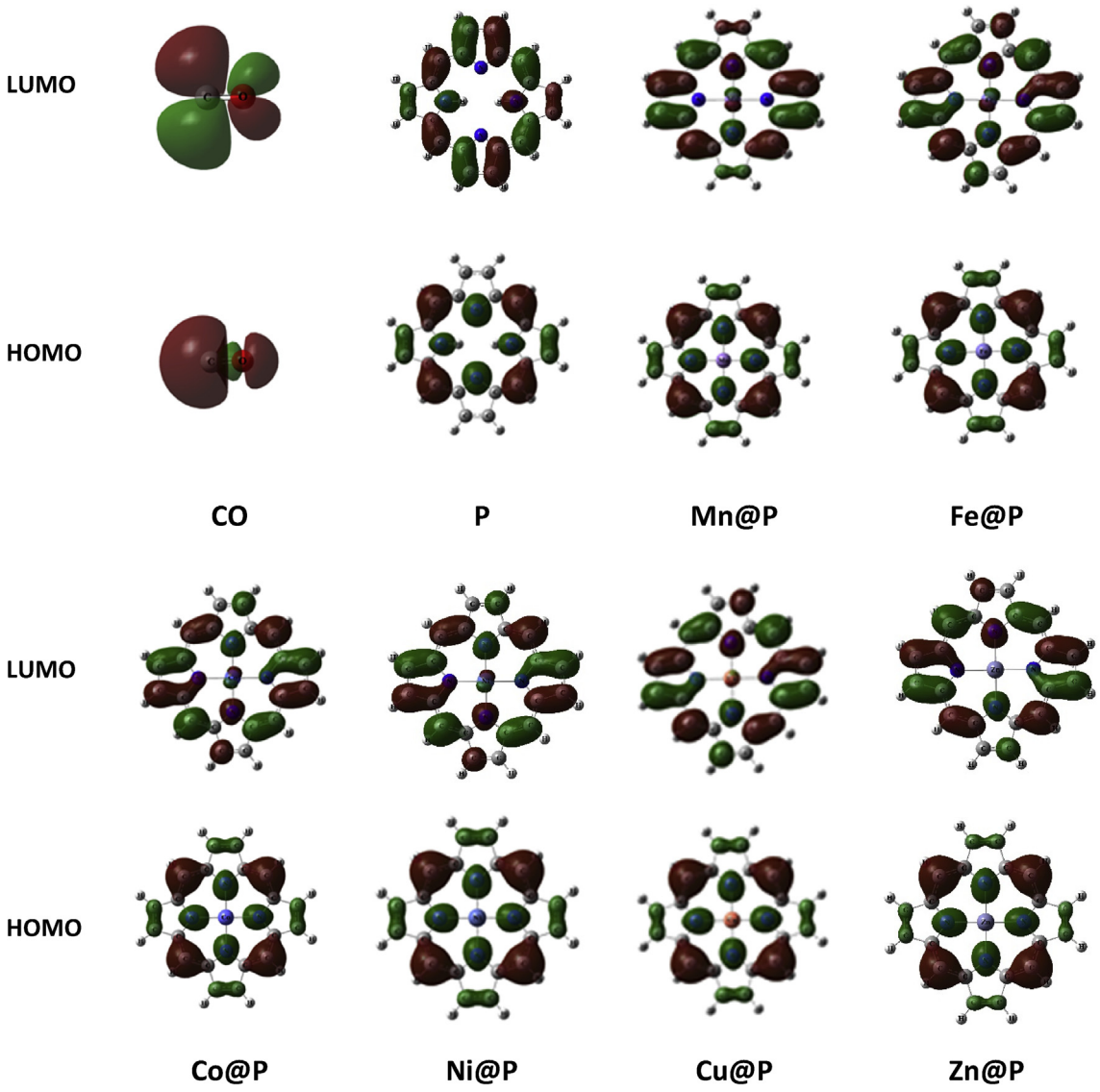

Fig. 5. HOMO and LUMO diagrams calculated at B3LYP/LanL2DZ for free CO molecule, bare P, and TM@P.

for mode 1 are in the range of -0.102 to -1.042 eV and -0.078 to -0.756 eV while for mode 2 are in the range of -0.056 to -0.131 eV and -0.044 to -0.093 eV for LanL2dz and 6-31G(d) basis sets, respectively. So one can say that, mode 1 for CO adsorption on TM@P is more preferable than mode 2. In mode 1, as the negative value of adsorption energies (E_{ads}) increases the distance ($d_{CO\text{-}TM}$) between CO molecule and the TM atom decreases. The adsorption nature depends on the species of TM where, it is chemisorption in nature in the cases of CO/Mn@P, CO/Fe@P, and CO/Co@P and physisorption in nature in the cases of CO/Ni@P, CO/Cu@P, and CO/Zn@P. On the other side, in mode 2 the adsorption nature is physisorption in nature for all TM species. Our results in good agreement with previous works. Shalabi et al [3], El-Gharkawy and Ammar [2], report that the CO molecule prefers to interact with the TM via its carbon head, where its carbon atom is a nucleophilic agent [28, 29]. Biesaga et al. [30] reported that Mn, Fe, and Co metalloporphyrins able to combine with two extra ligand molecules, Zn porphyrins able to combine with one extra ligand molecules, while Cu and Ni metalloporphyrins have generally low affinity for additional ligands. This explains the trend of CO adsorption in mode 2.

The local magnetic moments (μ) of the TM atom for TM@P and CO/TM@P were listed in Tables 1 and 3, respectively. One can notice in mode 1, the μ values decreased due to the CO adsorption for CO/Mn@P, CO/Fe@P, and CO/Co@P than those of Mn@P, Fe@P, and Co@P, while, the μ values have no significant changes for the rest complexes of mode 1 and all complexes in mode 2.

3.3. The NBO charge analysis

To understand the nature of CO interaction with P and TM@P, the natural bond orbital analysis were performed for CO/TM@P complexes to calculate atomic charges and electronic configurations. Since a larger basis sets are required for accurate charge transfer [31, 32, 33], LanL2DZ, 6-31G(d) as well as 6-311G(d) basis sets are utilized to calculate the atomic charges. As shown in Table 4, In mode 1, in the CO/Mn@P, and CO/Fe@P complexes, the positive charges on the TM atoms are decreased than those in TM@P complexes by 0.80, and 0.76 |e|, for LanL2DZ, 0.49, and 0.40 |e| for 6-31G(d), 0.41, and 0.33 |e| for 6-311G(d) respectively, see Table 1, while the CO molecule acquires a little charge values. These results guide one to suggest that due to CO adsorption a charge transfer takes place from the porphyrin molecule to the TM atom and this may explain the chemisorption nature in these cases. Looking to Table 5, it is noticed that the adsorption of CO molecule on CO/Mn@P, CO/Fe@P, and CO/Co@P leads to a change of the charge in the TM 3d-orbital by 0.57, 0.51, and 0.09 |e| for LanL2DZ, 0.13, 0.20,

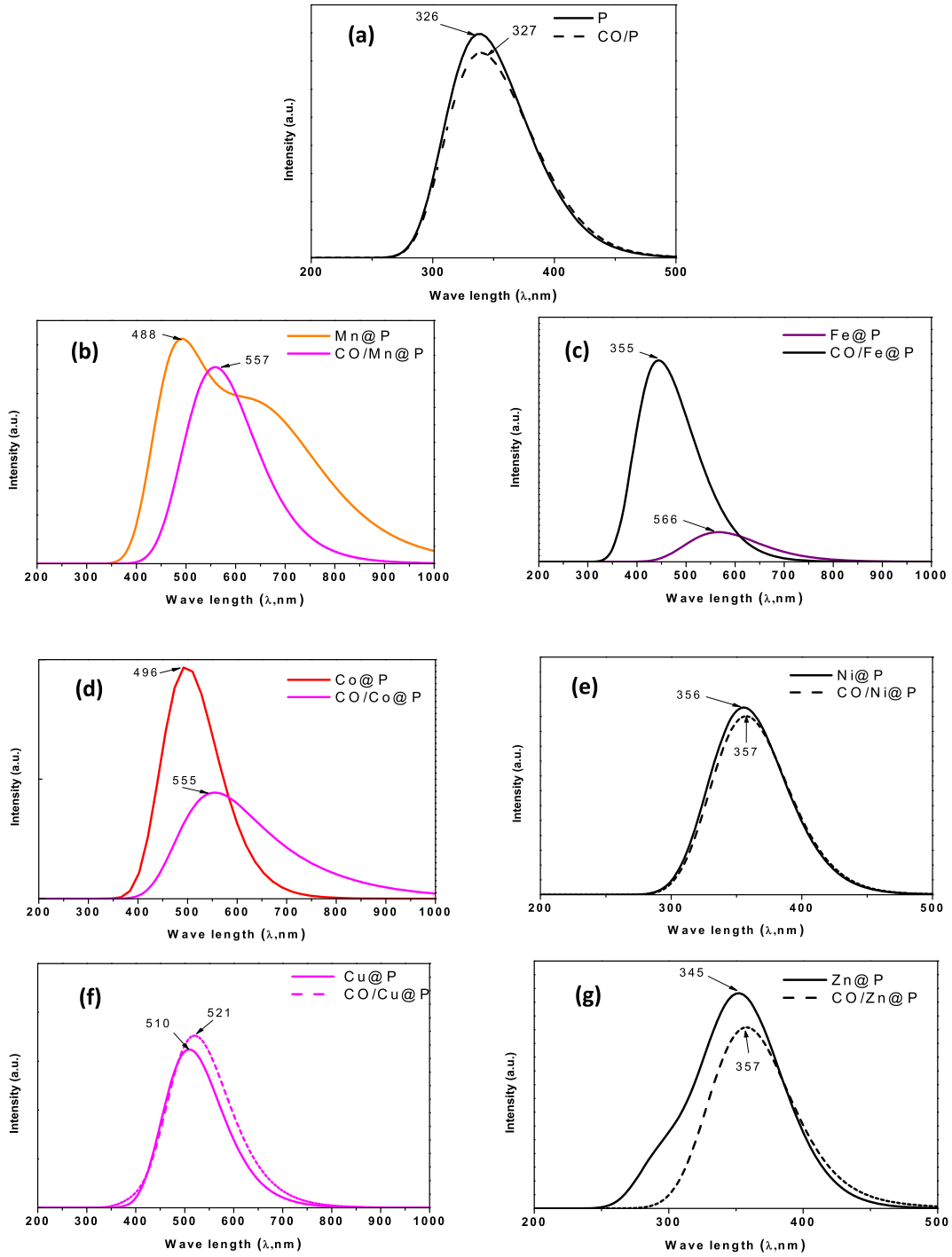

Fig. 6. Calculated absorption spectra at B3LYP/LanL2dz for (a) P, CO/P, (b) Mn@P, CO/Mn@P (c) Fe@P, CO/Fe@P (d) Co@P, CO/Co@P (e) Ni@P, CO/Ni@P (f) Cu@P, CO/Cu@P (g) Zn@P, CO/Zn@P

and -0.02 |e| for 6-31G(d), 0.38, 0.28, and 0.01 |e| for 6-311G(d), respectively. At the same time, it leads to deficiency of the charge in the CO carbon 2*s* orbital by 0.54, 0.55, and 0.27 |e|, for LanL2DZ, 0.13, 0.20, and -0.02 |e| for 6-31G(d), 0.38, 0.28, and 0.01 |e| for 6-311G(d), respectively, and growing the charge in the CO carbon 2p orbital by 0.26, 0.22, and 0.09 |e|, for LanL2DZ, 0.44, 0.40, and 0.22 |e| for 6-31G(d), 0.37, 0.33, and 0.18 |e| for 6-311G(d), respectively. While a negligible change in the electronic configuration of CO oxygen atom was observed. This encourage us to say that the interaction between CO molecules with TM@MP is attributed to donation-back donation as well as charge transfer mechanisms. On the other hand, the charge transfer in the adsorption mode 2 and the rest cases of adsorption mode 1 is very little and this may explain the physisorption nature in these cases.

3.4. DOS analysis

In this section, density of states (DOS) analysis was accomplished to study the role of dopant and CO adsorption on the electronic properties of the porphyrin. The DOS of CO, P and CO/P (Fig. 4a), TM@P (Fig. 4b), and CO/TM@P (Fig. 4c) are plotted where spin up (α) and down (β) are shown. Here, the most stable adsorption mode 1 are chosen.

HOMO and LUMO energy levels are calculated and listed in Tables 1,

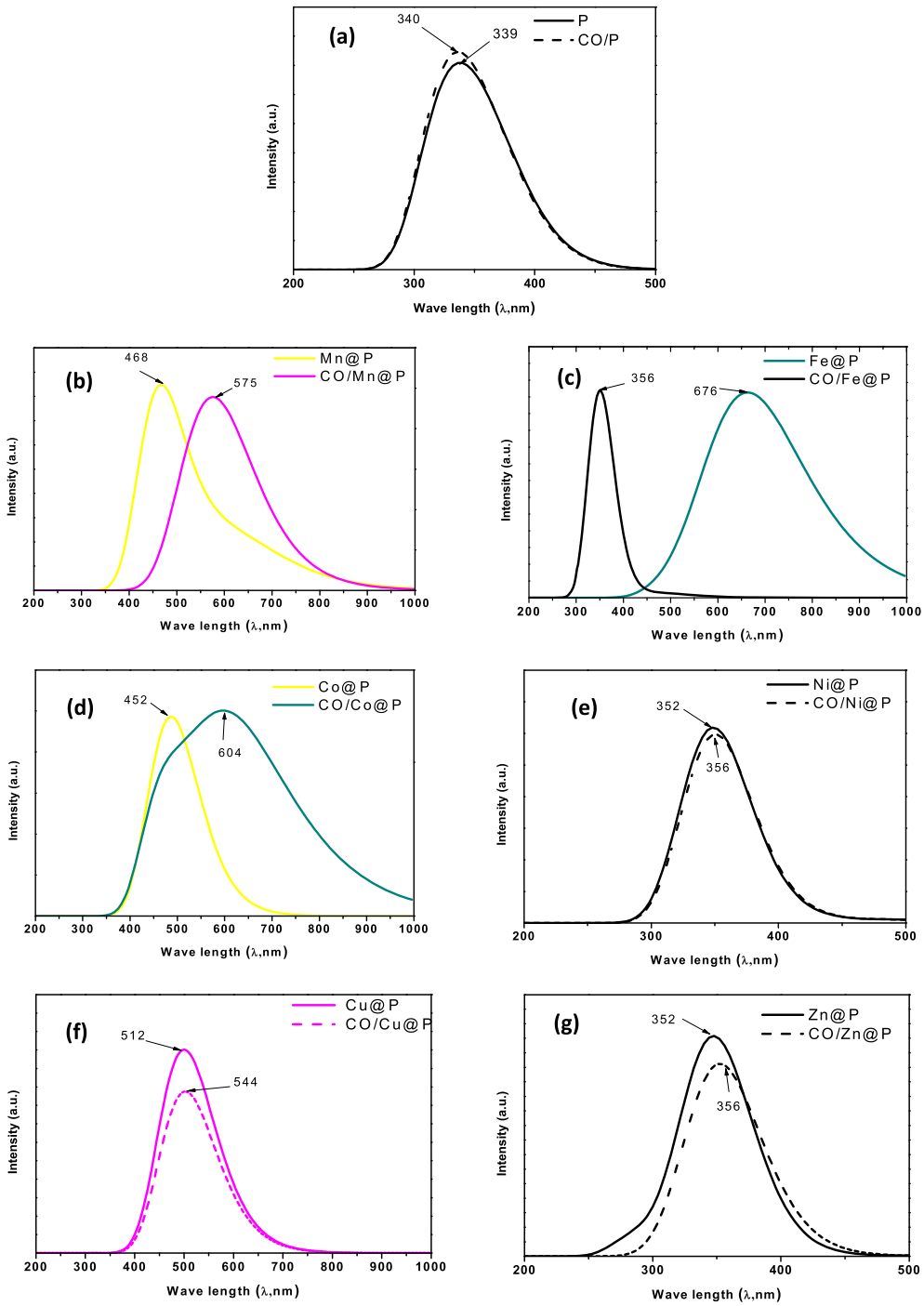

Fig. 7. Calculated absorption spectra at B3LYP/6-31G(d) for (a) P, CO/P, (b) Mn@P, CO/Mn@P (c) Fe@P, CO/Fe@P (d) Co@P, CO/Co@P (e) Ni@P, CO/Ni@P (f) Cu@P, CO/Cu@P (g) Zn@P, CO/Zn@P

2, and 3 for TM@P, CO/P, and CO/TM@P, respectively and depicted in Fig. 5. From Fig. 4a it is shown that porphyrin is a semiconductor material with HOMO-LUMO gaps of 2.8 eV and, which is in good agreement with Hamad et al. [34]. Due to the adsorption of CO on P the occupied states peak of the CO molecule is shifted from -10.3 to -9.7 eV, while no significant change is observed in the HOMO-LUMO gap of CO/P.

From Fig. 4b, it is clear that the TM doping atoms slightly lowering the HOMO and rising the LUMO energy levels of porphyrin. This in turn led to an increase ranging from 4.1% to 10.4% in the HOMO-LUMO gap of porphyrin.

By comparing the DOS for the TM in TM@P substrates and CO/TM@P complexes, in Fig. 4b and c, respectively, one can see that the peaks for Mn at -8.8, -8.2 and -7.7 eV in Mn@P are disappeared in CO/Mn@P complex. The peaks for Fe at -9.0, -7.9 and -7.4 eV in Fe@P are disappeared in CO/Fe@P complex. The peaks for Co at -7.8, and -6.4 eV in Co@P are shifted in CO/Co@P complex. In contrast, there is no noticeable changes in the DOS of Ni, Cu and Zn atom due to the CO adsorption. This may explains the higher adsorption in CO/Mn@P, CO/Fe@P and CO/Co@P complexes than CO/Ni@P, CO/Cu@P and CO/Zn@P complexes. In addition, the adsorption of CO on TM@P has a negligible effect on HOMO-LUMO gap of porphyrin and led to a change ranging from -6.94% to 3.45% of TM@P complexes.

It is well known that the HOMO-LUMO gap (E_g) is a major factor for determination of the electrical conductivity of a material, the classical relation between them is as follows [35]:

$$\sigma \ \alpha \ \exp\left(\frac{-E_g}{2kT}\right) \quad (8)$$

where, $\sigma$is the electrical conductivity and k is the Boltzmann's constant.

It is clear that the CO adsorption on both of P and TM@P has not a noticeable change on their electric conductivity. As a result, it is not suggested to use TM@P complexes as an electrochemical gas sensor for CO.

3.5. UV spectra analysis

To study the effect of TM doping and CO adsorption on the optical properties of the porphyrin, TD-DFT calculations were performed for P, TM@P, CO/P, and CO/TM@P based on their optimal structures to simulate their UV-Vis absorption spectra and shown in Figs. 6 and 7 for calculations at B3LYP/LanL2dz and B3LYP/6-31G(d) levels of theory, respectively. It was found that absorption peaks calculated by LanL2dz and 6-31G(d) basis sets of porphyrin (326 and 340 nm), Fe@P (355 and 356 nm), Ni@P (356 and 352 nm) and Zn@P (345 and 352 nm), respectively, identify them as ultra-violet active compounds, while, Mn@P (488 and 468 nm), Co@P (496 and 452 nm) and Cu@P (510 and 512 nm) are found to be active in the visible range of electromagnetic spectra. On the other hand, absorption peaks of CO/P (327 and 339 nm), CO/Ni@P (357 and 356 nm) and CO/Zn@P (357 and 356 nm) identify them as ultra-violet active compounds, CO/Mn@P (557 and 575 nm), CO/Fe@P (566 and 676 nm), CO/Co@P (555 and 604 nm) and CO/Cu@P (521 and 544 nm) are found to be active in the visible range of electromagnetic spectra. One can conclude that the adsorption of CO molecule on Mn@P, and Co@P, leads to a considerable shift in their visible light absorption beaks and CO adsorption on Fe@P converts it from ultra-violet active compounds to visible active compound. Finally, according to our results some species of TM-doped porphyrins (Mn@P, Co@P, and Fe@P) are optically sensitive to CO gas.

4. Conclusion

The calculation results at the B3LYP/LanL2dz and B3LYP/6-31G(d) levels of theory showed that both of P and TM@P; TM = Mn, Fe, Co, Ni, Cu, and Zn molecules are planar. Two adsorption modes were suggested for CO molecule on P and TM@P. The CO molecule prefers to interact with P and TM@P via its carbon head. The binding of the CO gas molecules onto the porphyrin is mainly due to electrostatic and van der Waals interactions and it is physisorption in nature. The CO adsorption nature on TM@P substrates depends on two factors, the orientation of CO molecule as well as the species of the doping TM. The presence of Mn, Fe, Co, and Zn enhances the adsorption of CO molecule. The CO adsorption on both of P and TM@P has not a noticeable change on their electric conductivity. As a result, it is not suggested to use TM@P complexes as an electrochemical gas sensor for CO. According to the TD-DFT calculation results, some species of TM-doped porphyrins (Mn@P, Co@P, and Fe@P) are optically sensitive to CO gas.

Declarations

Author contribution statement

H. Y. Ammar, H.M. Badran: Conceived and designed the experiments; Performed the experiments; Analyzed and interpreted the data; Contributed reagents, materials, analysis tools or data; Wrote the paper.

Funding statement

This research did not receive any specific grant from funding agencies in the public, commercial, or not-for-profit sectors.

Competing interest statement

The authors declare no conflict of interest.

Additional information

No additional information is available for this paper.

References

[1] T. Ouyang, Z. Qian, R. Ahuja, X. Liu, First-principles investigation of CO adsorption on pristine, C-doped and N-vacancy defected hexagonal AlN nanosheets, Appl. Surf. Sci. 439 (2018) 196–201.
[2] E.R.H. El-Gharkawy, H.Y. Ammar, Adsorption of CO on TM-deposited $(MgO)_{12}$ nano-Cage (TM = Ni, Pd and Pt): a study on electronic properties, J. Nanoelectron. Optoelectron. 13 (2018) 546–553.
[3] A.S. Shalabi, S. Abdel Aal, M.A. Kamel, H.O. Taha, H.Y. Ammar, W.S. Abdel Halim, The role of oxidation states in F_{A1} Tl^{n+} (n = 1,3) lasers and CO interactions at the (100) surface of NaCl: an ab initio study, Chem. Phys. 328 (2006) 8–16.
[4] J. Chen, Q. Ma, X. Hu, Y. Gao, X. Yan, D. Qin, X. Lu, Design of a novel naked-eye and turn-on fluorescence sensor based on the 5,10,15,20-(4-sulphonatophenyl) porphyrin (TPPS4)-Hg^{2+} system: monitoring of glutathione (GSH) in real samples and DFT calculation, Sens. Actuators B 254 (2018) 475–482.
[5] S. Kumar, de A.E. Silva, M.Y. Wani, J.M. Gil, Carbon dioxide capture and conversion by an environmentally friendly chitosan based meso-tetrakis (4-sulfonatophenyl) porphyrin, Carbohydr. Polym. 175 (2017) 575–583.
[6] K.M. Kadish, K.M. Smith, R. Guilard, Handbook of Porphyrin Science, WorldScientific, 2010.
[7] Z. Li, P. Dong, R.P. Liang, J.D. Qiu, Nitrogen-doped graphene quantum dots as anew catalyst accelerating the coordination reaction between cadmium(II) and 5,10,15,20-tetrakis (1-methyl-4-pyridinio) porphyrin for cadmium(II) sensing, Anal. Chem. 87 (2015) 10894–10901.
[8] P.K. Palomaki, M.R. Civic, P.H. Dinolfo, Photocurrent enhancement by multi layered porphyrin sensitizers in a photoelectrochemical cell, ACS Appl. Mater. Interfaces 5 (2013) 7604–7612.
[9] Y. Hu, Z. Xue, H. He, R. Ai, X. Liu, X. Lu, Photoelectrochemical sensing for hydroquinone based on porphyrin-functionalized Au nanoparticles on graphene, Biosens. Bioelectron. 47 (2013) 45–49.
[10] D.E. Bikiel, S.E. Bari, F. Doctorovich, D.A. Estrin, DFT study on the reactivity of iron porphyrins tuned by ring substitution, J. Inorg. Biochem. 102 (2008) 70–76.
[11] S. Bhandary, B. Brena, P.M. Panchmatia, I. Brumboiu, M. Bernien, C. Weis, B. Krumme, C. Etz, W. Kuch, H. Wende, O. Eriksson, B. Sanyal, Manipulation of spin state of iron porphyrin by chemisorption on magnetic substrates, Phys. Rev. B 88 (2013), 024401.
[12] D.R. Roy, E.V. Shah, S.M. Roy, Optical activity of Co-porphyrin in the light of IR and Raman spectroscopy: a critical DFT investigation, Spectrochim. Acta A Mol. Biomol. Spectrosc. 190 (2018) 121–128.
[13] S. Paul, F. Amalraj, S. Radhakrishnan, CO sensor on polypyrrole functionalized with iron porphyrin, Synth. Met. 159 (2009) 1019–1023.
[14] Y. He, J. Zhang, J. Zhao, Electron transport and CO sensing characteristics of Fe(II) Porphyrin with single-walled carbon nanotube electrodes, J. Phys. Chem. C 118 (2014) 18325–18333.
[15] F. Mosciano, G. Magna, A. Catini, G. Pomarico, E. Martinelli, R. Paolesse, C. Di Natale, Room temperature CO detection by hybrid porphyrin-ZnO nanoparticles, Procedia Eng. 120 (2015) 71–74.
[16] Y.H. Chang, H. Kim, S. Kahng, Y. Kim, Axial coordination and electronic structure of diatomic NO, CO, and O_2 molecules adsorbed onto Co-tetraphenylporphyrin on Au(111), Ag(111), and Cu(111): a density-functional theory study, Dalton Trans. 45 (2016) 16673–16681.
[17] S. Lian, M.S. Kodaimati, E.A. Weiss, Photocatalytically active superstructures of quantum dots and iron porphyrins for reduction of CO_2 to CO in water, ACS Nano 12 (2018) 568–575.
[18] E.V. Shah, V. Kumar, B.K. Sharma, K. Rajput, V.P. Chaudhary, D.R. Roy, Co-Tetraphenylporphyrin (co-TPP) in TM-TPP (TM = Fe, Co, Ni, Cu, and Zn) series: a new optical material under DFT, J. Mol. Model. 24 (2018) 239.
[19] M. Liao, S. Scheinera, Electronic structure and bonding in metal porphyrins, Metal=Fe, Co, Ni, Cu, Zn, J. Chem. Phys. 117 (2002) 205–219.
[20] W. Kohn, L. Sham, self-consistent equations including exchange and correlation effects, Phys. Rev. A 140 (1965) 1133.
[21] M.J. Frisch, et al., Gaussian 09, Revision D.01, Gaussian, Inc., Wallingford, CT, 2009.
[22] N.M. O'Boyle, A.L. Tenderholt, K.M. Langner, cclib, A library for package-independent computational chemistry algorithms, J. Comput. Chem. 29 (2008) 839–845.
[23] E.D. Glendening, A.E. Reed, J.E. Carpenter, F. Weinhold, NBO Version 3.1.
[24] R. Giovannetti, Available from:, in: Jamal Uddin (Ed.), The Use of Spectrophotometry UV-Vis for the Study of Porphyrins, Macro to Nano Spectroscopy, InTech, 2012 http://www.intechopen.com/books/macro-to-nano-spectroscopy/the-use-of-spectrophotometry-uv-vis-for-thestudy-of-porphyrins.

[25] M. Yang, Y. Zhang, S. Huang, H. Liu, P. Wang, H. Tian, Theoretical investigation of CO adsorption on TM-doped (MgO)12 (TM=Ni, Pd, Pt) nanotubes, Appl. Surf. Sci. 258 (2011) 1429–1436.
[26] I.M. Soliman, M.M. El-Nahass, Kh.M. Eid, H.Y. Ammar, Vibrational spectroscopic analysis of aluminum phthalocyanine chloride. Experimental and DFT study, Physica B 491 (2016) 98–103.
[27] N. Norman Greenwood, A. Earnshaw, Chemistry of the Elements, second ed., Butterworth-Heinemann, Oxford, 1997, p. 700.
[28] P. Politzer, C.W. Kammeyer, J. Bauer, W.L. Hedges, [1.1.1] Propellane, bicyclo [1.1.1] pentane and the effects of "inverted" carbons, J. Phys. Chem. 85 (1981) 245–252.
[29] G. Frenking, C. Loschen, A. Krapp, S. Fau, S.H. Strauss, Electronic structure of CO-an exercise in modern chemical bonding theory, J. Comput. Chem. 28 (2006) 117–126.
[30] M. Biesaga, K. Pyrzyńska, M. Trojanowicz, Porphyrins in analytical chemistry, Review, Talanta 51 (2000) 209–224.
[31] Saif Ullah, P.A. Denis, F. Sato, Beryllium doped graphene as an efficient anode material for lithium-ion batterieswith significantly huge capacity: a DFT study, Appl. Mater. Today 9 (2017) 333–340.
[32] Saif Ullah, P.A. Denis, F. Sato, First-principles study of dual-doped graphene: towards promising anode materials for Li/Na-ion batteries, New J. Chem. 42 (2018) 10842–10851.
[33] Saif Ullah, P.A. Denis, F. Sato, Triple-doped monolayer graphene with boron, nitrogen, aluminum, silicon, phosphorus, and sulfur, ChemPhysChem 18 (2017) 1864–1873.
[34] S. Hamad, N.C. Hernandez, A. Aziz, A.R. abdel Ruiz-Salvador, S. Calero, R. Grau-Crespo, Electronic structure of porphyrin-based metal–organic frameworks and their suitability for solar fuel production photocatalysis, J. Mater. Chem. 3 (2015) 23458–23465.
[35] S. Li, Semiconductor Physical Electronics, second ed., Springer, USA, 2006.